HAL
open science

Controlled elaboration of large-area plasmonic substrates by plasma process

Alessandro Pugliara, Caroline Bonafos, Robert Carles, Bernard Despax, Kremena Makasheva

To cite this version:

Alessandro Pugliara, Caroline Bonafos, Robert Carles, Bernard Despax, Kremena Makasheva. Controlled elaboration of large-area plasmonic substrates by plasma process. Materials Research Express, 2015, 2 (6), 10.1088/2053-1591/2/6/065005 . hal-01763544

HAL Id: hal-01763544

https://hal.science/hal-01763544v1

Submitted on 2 Sep 2022

HAL is a multi-disciplinary open access archive for the deposit and dissemination of scientific research documents, whether they are published or not. The documents may come from teaching and research institutions in France or abroad, or from public or private research centers.

L'archive ouverte pluridisciplinaire **HAL**, est destinée au dépôt et à la diffusion de documents scientifiques de niveau recherche, publiés ou non, émanant des établissements d'enseignement et de recherche français ou étrangers, des laboratoires publics ou privés.

Controlled elaboration of large-area plasmonic substrates by plasma process

A. Pugliara,[1,2] C. Bonafos,[2] R. Carles,[2] B. Despax[1] and K. Makasheva[1,a)]

[1]LAPLACE (Laboratoire Plasma et Conversion d'Energie), Université de Toulouse; CNRS, UPS, INPT; 118 route de Narbonne, F-31062 Toulouse cedex 9, France
[2]Groupe Nanomat-CEMES (Centre d'Elaboration de Matériaux et d'Etudes Structurales)-CNRS; Université de Toulouse, 29 rue Jeanne Marvig, BP 94347, F-31055 Toulouse cedex 4, France

[a)]Corresponding author: kremena.makasheva@laplace.univ-tlse.fr
Keywords: Silver nanoparticles, plasmonic substrates, PECVD, PVD, plasma silica.

Abstract
Elaboration in a controlled way of large-area and efficient plasmonic substrates is achieved by combining sputtering of silver nanoparticles (AgNPs) and plasma polymerization of the embedding dielectric matrix in an axially-asymmetric capacitively-coupled RF discharge maintained at low gas pressure. The plasma parameters and deposition conditions were optimized according to the optical response of these substrates. Structural and optical characterizations of the samples confirm the process efficiency. The obtained results indicate that to deposit a single layer of large and closely situated AgNPs a high injected power and short sputtering times must be privileged. The plasma elaborated plasmonic substrates appear very sensitive to any stimuli that affect their plasmonic response.

1. Introduction

The properties of nanocomposite materials are nowadays widely studied aiming at a large spectrum of applications. Nanocomposite materials consisting of noble metallic nanoparticles embedded in dielectric matrix represent a huge interest for plasmonic devices to manipulate, localize and enhance the electromagnetic field at nanoscale level [1]. The plasmonic coupling with light enhances the range of useful optical phenomena having potential applications in areas such as ultra-sensitive chemical and biomolecular detection, enhanced spectroscopies, photocatalysis, *etc*.

It is generally acknowledged that silver nanoparticles (AgNPs) realize the best nanoscale antenna for amplifying local electronic and vibrational signals in the visible range, providing unique molecular information in the optical far-field regime. In the field of scientific research, two main spectroscopy techniques have emerged based on Localized Surface Plasmon Resonance (LSPR) and Surface-Enhanced Raman Scattering (SERS). Advances in micro and nano-fabrication technology have made available integration of sensitive LSPR to lab-on-a-chip platforms. They are increasingly popular in fundamental biological studies, health science research and environmental monitoring [2-4]. Since its discovery in 1974 on pyridine molecules adsorbed on rough silver surfaces [5], SERS has received a great deal of attention as powerful analytical technique for molecular spectroscopy, biomolecular recognition and ultra-sensitive detection (down to a single molecule). However, the limits imposed by the fabrication of SERS substrates remain the major drawback for their large application. It is due to the drastic requirements for controlling on large area, and in a reproducible way, a well-defined spacing between the metallic nanostructures and the probing molecules. Generally, the enhancement of the scattering cross-section for SERS substrates is attributed to an electromagnetic mechanism (based on surface “plasmon resonance”) and/or to a chemical one (based on “charge transfer”). Whatever the mechanism, the requirement for an efficient SERS substrate is the fine control on nanometer scale of size and shape of the metallic particles, and of the distance between their surface and the probed molecules. As a consequence, another challenge to overcome is control of the thickness and porosity of the coverlayer. The thickness of the coverlayer must be selected at nanoscale level as a compromise between the preservation of SERS enhancement and the protection of AgNPs against oxidation, for example [6], and against direct interaction of the AgNPs with the probing molecules [4].

Development of solid SERS substrates based on metal nanostructures covered by a polymer [7], or by inorganic materials (ultrathin SiO_2 layers) [8] allowed improving their stability and performance. The SiO_2-coated SERS substrates proved to be especially useful in SERS-based biosensors because of the well-defined hydrophilic and stabilizing properties which actually motivated the current study. Different elaboration methods have been applied for the synthesis of solid SERS substrates. The explored ways are either via chemical reactions, lithographic fabrication, and template-direct growth [2, 3 and the references therein], via thermal evaporation [8] or more recently via low energy ion implantation beam synthesis (LE-IBS) [9-11], all of them emphasizing the large interest for applications and the importance of strict control during the synthesis of SERS substrates.

Plasma based deposition processes are known to be quite versatile for deposition of nanocomposite thin layers containing metal clusters. Intensive research on the possibilities to obtain thin nanocomposite layers sustained of metallic nanoparticles embedded in dielectric matrices started with the works of E. Kay *et al*. [12] where Physical Vapor Deposition (PVD) and Plasma Enhanced Chemical Vapor Deposition (PECVD) were combined in one process to obtain gold nanoparticles dispersed in fluorocarbon matrices. This approach, privileged also by other research groups [12-20], offers several advantages compared to other deposition techniques. It allows: (*i*) a quite easy control of the metal content in the thin film only by controlling the partial pressures of the plasma feeding gas and the gas precursors in the discharge, leading to the possibility to obtain materials with metallic concentration from a few percent up to 100%; (*ii*) homogeneous dispersion of the metal nanoparticles in the film and (*iii*) fine control over the size of the metal nanoparticles.

Optical properties of this type of nanocomposite structures can finely be tuned by simply varying the metal volume fraction in the layer [13]. Strong structural modifications of both the metal nanoparticles and the surrounding matrix can be achieved by thermally induced processes occurring in the plasma gas phase and/or by post-deposition annealing [13-15]. Stability of the plasma elaborated host matrix to exposure to different aging agents (air, aqueous media, *etc*.) is shown to be superior for amorphous hydrophilic matrices (plasma silica – a-SiO_2, organosilicon – a-SiOC:H or oxygenated hydrocarbon – a-CH:O) compared to amorphous hydrophobic ones (fluorocarbon – a-F-C or hydrocarbon – a-C-H) [13-20]. Although the stability of amorphous hydrophilic matrices is generally good, the more resistant matrix is the silica, compared to organosilicon or oxygenated hydrocarbon matrices, as it is the densest one. Moreover, release of metallic ions and/or metallic nanoparticles from the plasma mediated nanocomposite thin films, in particular Ag^+ and AgNPs [20-25], shows dependence on the size and density of metal nanoparticles and on the type of the host dielectric matrix (hydrophilic/hydrophobic properties and porosity) and the distance from the AgNPs to the substrate surface. Additionally to the possibility of large variation of the optical, structural and electrical properties of the nanocomposites, offered by the above described plasma process, the stability related issues must be considered when a given application of the nanocomposite thin films is pursued.

This work presents results on plasma deposition process for elaboration in a controlled way of large-area plasmonic substrates consisted of a single layer of AgNPs deposited on SiO_2 layer and coated by ultrathin SiO_2 plasma layer. The plasma process and details on the operation conditions are given in the next section. Diagnostic methods applied for the structural and optical characterization (TEM, FTIR, ellipsometry and reflectometry) of the elaborated substrates and results from their analysis along with the discussion are presented in Section 3. The functionality of the elaborated plasmonic substrates is demonstrated on the basis of their optical response in ellipsometry and reflectometry measurements. Finally, Section 4 summarizes the main conclusions and gives the perspectives.

2. Plasma deposition process

The purpose in this part of the study is to elaborate nanocomposite structures of SiO_2/AgNPs/SiO_2/Si (a single layer of AgNPs, with well controlled size, density and distance among the nanoparticles, is inserted in a SiO_2 matrix at a given distance from the surface)

with highly pronounced anti-reflective properties. The thickness of the whole structure must be selected in a way that for specific wavelengths the reflectance is at minimum and consequently the electric field at the free surface is at maximum, as accounted for by modelling the propagation of electromagnetic waves in stratified media [10,11]. In the current study a total thickness of 100 nm of the nanocomposite structure was intended.

The nanocomposite structures were elaborated by using the plasma of an axially-asymmetric capacitively-coupled RF (13.56 MHz) discharge combing PVD, as a first step, and PECVD as a second step in the applied deposition procedure shown in Fig. 1. The discharge powered electrode (smaller electrode) was an Ag-made target to bear the silver sputtering. The axially-asymmetric design of this RF discharge induces a self-bias voltage V_{dc} on the powered electrode, controlling in that way the metal sputtering. Deposition of plasma silica coverlayer was performed in the same reactor. The plasma reactor is described in details elsewhere [16]. The plasma behaviour during deposition was controlled by Optical Emission Spectroscopy (OES) and electrical measurements. For both deposition steps – sputtering and plasma polymerization – variation of the $I_{Ag(546.6nm)}/I_{Ar(549.6nm)}$ ratio as a function of the injected power or the gas mixture composition was recorded. This kind of chart constitutes useful data to obtain reproducible results [16].

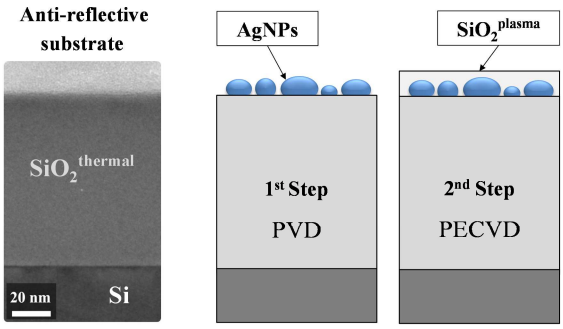

Figure 1. Pathway for elaboration of large-area plasmonic substrates (single layer of AgNPs embedded in SiO_2 matrix) by plasma process.

The used plasma process is fully compatible with the standard microelectronic technologies. As discussed above it is versatile in terms of experimental conditions which enlarges the possibility to probe and, consequently, to optimize the optical response of the elaborated plasmonic structures. To realize the plasmonic structures a single layer of AgNPs was deposited by Ag-sputtering on the surface of thermally grown SiO_2-layer (thickness of 80 nm) on Si-substrate (2” in diameter) in Ar-discharge maintained at low gas pressure (p_{Ar} = 5.2 Pa). The substrate was fixed to the grounded electrode. It was previously cleaned in Piranha solution for 2 min, followed by chemical etching for 30 seconds in hydrofluoric acid (HF). At each step of the cleaning procedure the substrates were rinsed with deionized water. The cleaning procedure is indispensable for the elaboration of plasmonic substrates because it guarantees the removal of the surface contamination and the native oxide, known to be badly organized from structural point of view and presenting poor electrical properties.

The AgNPs size, density and shape were controlled through tuning the sputtering operating conditions. The sputtering time was varied between 5 s and 30 s for different input powers (P = 10 – 80 W), corresponding to a self-bias voltage variation in the range V_{dc} = -

400 – -1000 V (Fig. 2a). The plasma process was monitored by OES through the ratio of $I_{Ag(546.6nm)}$ to $I_{Ar(549.6nm)}$ line intensities. For the sputtering step the evolution of $I_{Ag(546.6nm)}/I_{Ar(549.6nm)}$ ratio gives an image of the Ag amount in the plasma which can be related to the Ag volume fraction deposited on the substrate. Figure 2a shows the measured self-bias voltages as a function of the applied power during the Ag-sputtering and the corresponding line intensity ratio of the silver line $I_{Ag(546.6nm)}$ to the argon line $I_{Ar(549.6nm)}$. Previous to each sputtering the Ag-target was mechanically polished, then cleaned in the Ar-discharge and the plasma process stability was followed by OES. When the emission spectrum from the plasma (Fig. 2b), and in particular the $I_{Ag(546.6nm)}/I_{Ar(549.6nm)}$ ratio, was found to be constant throughout at least 5 minutes the Ag-sputtering was performed. During the plasma stabilization phase the substrate was hidden behind a shutter [16]. Ones the plasma process stability was attained, typically about 10 minutes are needed for the sputtering step, the shutter was removed for the time of sputtering. The possibility to hide the substrate during the plasma stabilization phase, and ones the Ag-sputtering step has been performed, allows us to use very short deposition times (only of few seconds) and to obtain a strict control of the plasma deposition process.

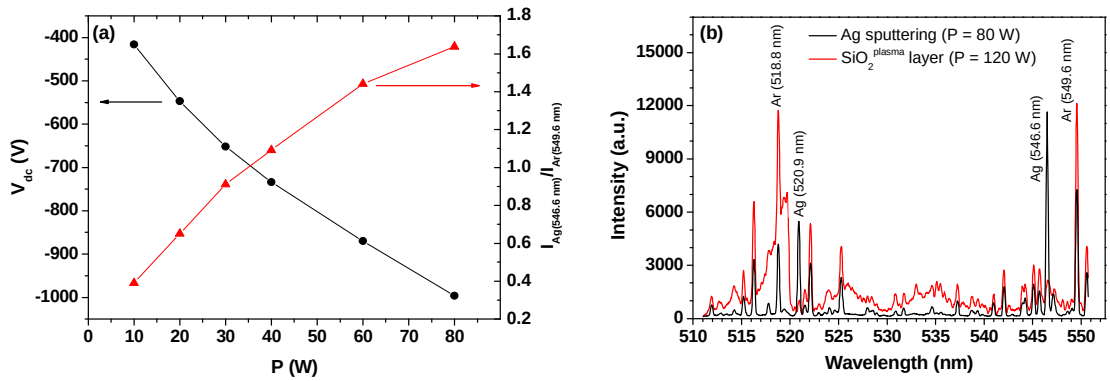

Figure 2. (a) Evolution of the self-bias voltage V_{dc} and the ratio of the line intensities $I_{Ag(546.6nm)}$ to $I_{Ar(549.6nm)}$ as a function of the applied discharge power during the sputtering step (p_{Ar} = 5.2 Pa) and (b) OES spectra from the plasma sustained in Ar at p_{Ar} = 5.2 Pa and P = 80 W during the Ag sputtering step (black curve) and of the plasma sustained in Ar/HMDSO/O_2 mixture at average total pressure p_{tot} = 7.68 Pa and P = 120 W for the SiO_2 plasma deposition step (red curve).

The plasma silica (SiO_2^{plasma}) coverlayer embedding the AgNPs was deposited in the plasma sustained in a gas mixture of argon (Ar flow - 2.8 sccm, where sccm stands for standard cubic centimeters) - hexamethyldisiloxane (HMDSO - $[CH_3]_6Si_2O$) - oxygen (O_2 flow – 1.25 sccm) at average total gas pressure p_{tot} = 7.68 Pa. The HMDSO (Sigma Aldrich product with purity larger than 99.5%) and argon (AirLiquid AlphaGaz 2 - 99.9995%) flows were mixed in a buffer chamber before being introduced into the plasma chamber. The high quality oxygen flow (AirLiquid AlphaGaz 2 - 99.9995%) was introduced into the plasma chamber by means of an appropriate port situated at the level of the grounded electrode where the substrate was fixed. Strong particularity of our plasma process which makes it original and highly efficient is the pulsed introduction of the precursor. The HMDSO was introduced in the discharge by pulses with period T = 5 s ($T = t_{on} + t_{off}$) and injection time t_{on} = 3.1 s which corresponds to an average HMDSO flow of 0.248 sccm. The maximal fluctuation of the total

gas pressure induced by the pulsed injection of the HMDSO was of 0.4 Pa. The combined effect of pulsed introduction of HMDSO in the plasma and the specific location of O_2 introduction, in the vicinity of the substrate, has finally a strong impact on the quality of the deposited SiO_2^{plasma} coverlayer. It allows deposition of high quality SiO_2 plasma layers for relatively low O_2 to HMDSO ratios. The injected RF power for the SiO_2^{plasma} deposition was fixed to 120 W assuring high degree of HMDSO decomposition in the plasma. Obtaining high quality SiO_2^{plasma} layers, in a plasma process by using HMDSO as precursor, requires diagnostic of the plasma parameters as a function the gas discharge operating conditions - type of gas discharge, injected power, gas pressure and gas mixture [26-30]. Once more, like in the Ag-sputtering step, previous to the SiO_2^{plasma} deposition the stability of plasma process was followed until obtaining constant values for the self-bias voltage, the total average gas pressure and the glow emission from the discharge for at least 5 minutes. For the SiO_2^{plasma} deposition step the plasma stabilization phase takes typically 30 minutes. All experiments for the SiO_2^{plasma} deposition were carried without any silver atomic presence in the plasma gas phase. This point was controlled through the absence of silver lines in the recorded optical emission spectra, like the example shown in Fig. 2b (red curve). It is worth to point here that the OES shown in Fig. 2b, corresponding to the plasma polymerization step, reflects the elementary processes occurring in the plasma gas phase. The thickness of the SiO_2^{plasma} coverlayer was controlled by the deposition time after a preliminary study on the deposition rate. The deposition rate, resultant from the above described plasma conditions, was found to be low, only of 13 nm/min. The low deposition rate used in this study gives place to deposition of a dense SiO_2^{plasma} coverlayer with well-ordered matrix. The SiO_2^{plasma} coverlayer should not only be of high quality (no C-H or Si-H content) but also exempt of any silver presence in it. In a preliminary study, where the optimization of the plasma operation conditions was performed, it was found that in the plasma of Ar-HMDSO-O_2 gas mixture, for HMDSO injection times larger than 3.0 s, over 5 s period, in the used in this study, axially-asymmetric capacitively-coupled RF discharge, the silver sputtering did not occur because of rapid plasma polymer covering of the silver electrode with a thin SiOC:H film. After each SiO_2^{plasma} deposition the plasma reactor walls and the Ag-target were cleaned, so that the initial conditions for the next deposition remained unchanged, guaranteeing in that way reproducibility of the elaborated plasmonic substrates.

3. Diagnostic methods for structural and optical characterization of the plasmonic substrates

Structural analysis of the elaborated plasmonic substrates was performed by Transmission Electron Microscopy (TEM) in plan and cross-section view, Fourier Transform InfraRed spectroscopy (FTIR) and ellipsometry. Cross-section and plan view specimens were prepared for TEM analyses by standard procedure using mechanical polishing followed by Ar^+ ion milling. The observations were performed using a field emission Transmission Electron Microscope, FEI Tecnai™ F20 microscope operating at 200 kV, equipped with a spherical aberration corrector. The FTIR spectra were acquired with a Brucker Vertex 70 spectrometer in the range 400 – 4000 cm^{-1} to obtain information about the composition of SiO_2^{plasma} deposited layer. The refractive index and thickness of the silica film were determined by spectroscopic ellipsometry using a SOPRA GES-5 ellipsometer in the range 250 – 850 nm

with an incident angle of 75°. The optical response of elaborated plasmonic substrates was analyzed on the basis of ellipsometry and reflectivity measurements. The reflectivity spectra were recorded by using a Varian Cary 5000 spectrophotometer in the range 200 – 800 nm in quasi normal incidence.

4. Results and discussion

Figure 3 represents a bright field TEM image in cross-section view of typical elaborated sample. It corresponds to the following structure: single layer of AgNPs deposited at injected power of P = 40 W for sputtering time of t_s = 5 sec and covered by SiO_2^{plasma} layer of thickness $d_{SiO2plasma}$ = 13 nm (deposition time for the SiO_2^{plasma} layer, t_d = 60 s). One can clearly notice the planarity in the AgNPs single layer (the AgNPs layer average thickness is of 9 nm). High Resolution Electron Microscopy (HREM) observations (see image in insert of Fig. 3) show that the Ag nanoparticles are crystalline and made of pure silver. The total thickness of the structure is 105 nm which fulfils the condition for anti-reflectivity of optical waves in the middle of the visible range [10,11].

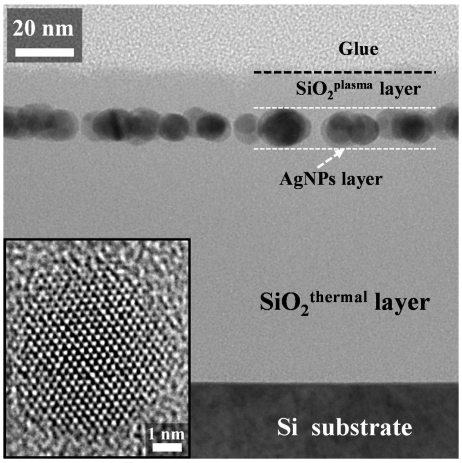

Figure 3. Bright field TEM cross-section image of a sample elaborated by combined silver sputtering and PECVD. Conditions for the AgNPs single layer deposition t_s = 5 s, P = 40W (V_{dc} = -750 V). The SiO_2^{plasma} deposition time, t_d = 60 s. In insert HREM image of a single nanocrystal.

The evolution of the AgNPs size, density and shape with the injected power for Ag-sputtering is shown in Fig. 4 for a fixed sputtering time t_s = 5 s and two different powers 40W (Fig. 4a) and 80W (Fig. 4b) covered by a SiO_2^{plasma} layer of thickness $d_{SiO2plasma}$ = 13 nm (SiO_2^{plasma} layer deposition time, t_d = 60 s). The size of AgNPs increases from 11.1 ± 2.4 nm to 19.6 ± 7.8 nm. Their density is reduced from 4.6×10^{11} NPs/cm^2 to 1.7×10^{11} NPs/cm^2, covering an area of 45.8% and 42.6%, respectively. The same trend is observed when the injected power is fixed and the sputtering time is increased. For P = 10 W, increasing the sputtering time from 10 s to 30 s leads to an increase of the mean diameter of the AgNPs from 4.5 ± 1.7 nm to 7.7 ± 2.8 nm corresponding to a coverage area of 13% and 19%, respectively. The density of AgNPs however decreases from 7.6×10^{11} NPs/cm^2 to 3.9×10^{11} NPs/cm^2, for the two sputtering times (t_s =10 s and t_s =30 s), respectively.

For a fixed sputtering time by scaling up the injected power the shape of AgNPs changes from spherical (P = 10 W) to prolate spheroid (P > 60 W). This property has been observed for other types of metal nanoparticles embedded in dielectric matrices, like Au-nanoparticles dispersed in fluorocarbon or hydrocarbon matrices, in the same type of gas discharges [13,14]. Increasing the sputtering time from 5 s up to 30 s does not influence the AgNPs shape for low injected power (P = 10 W), while it leads to overtaking the percolation threshold for high injected power (P = 80 W). Consequently, to obtain a single layer of large AgNPs, high injected power and small sputtering times must be privileged.

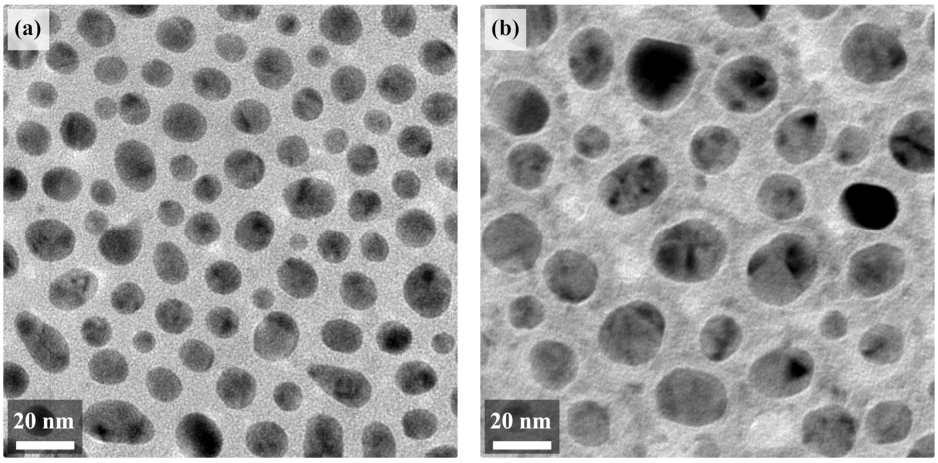

Figure 4. Bright field TEM plan-view images of the obtained plasmonic substrates by using different powers for the Ag-sputtering at fixed sputtering time t_s = 5 s: (a) 40W and (b) 80W.

As mentioned above, another challenge in the plasma elaboration of plasmonic substrates is the SiO_2 coverlayer. To achieve a SiO_2^{plasma} layer with properties close to thermal silica layer the plasma composition was adjusted by varying the gas mixture. The oxygen injection into the plasma maintained in Ar-HMDSO mixture introduces reactive species that promote oxidation of the methyl groups and the volatile species, such as water and carbon dioxide. To improve the oxidation efficiency in the plasma reactor used for this study, the oxygen flow was introduced grazing the surface of the samples by means of an appropriate port. The parameters for plasma polymerization phase, like applied power, HMDSO injection time and O_2 flow were optimized by OES and electrical measurements of the self-bias voltage. Typical OES spectrum of the plasma emission is shown in Fig. 2b. The real-time monitoring of the plasma process by OES [16] is indispensable for obtaining plasma silica layers of high quality.

The pulsed injection of the precursor is one of the originality of the applied plasma process. Indeed, pulsed injection of HMDSO allows fine control of the plasma parameters. The suitable HMDSO injection time was determined in relation with the O_2 flow in order to ensure both complete plasma organosilicon covering of the Ag-made electrode to prevent from Ag-sputtering and a plasma deposition of SiO_2 layer with properties close to a thermal silica layer. It was found that the slot of plasma operation parameters that satisfies the above two requirements for the quality of SiO_2^{plasma} layer is very narrow. To avoid Ag presence in the discharge, and consequently in the SiO_2^{plasma} layer, the HMDSO injection time must be longer than 3.0 s, over 5 s period, for the O_2 gas flows of 1.25 sccm. However, to prevent from possible C-H content in the SiO_2^{plasma} layer the HMDSO injection times must not be

longer than 3.2 s for the O_2 gas flows of 1.25 sccm. The composition of deposited SiO_2 layer was determined by FTIR and ellipsometry. It is in accordance with the SiO_2 layers obtained by other authors using O_2 and HMDSO as precursors for silica deposition in a plasma process [28-30].

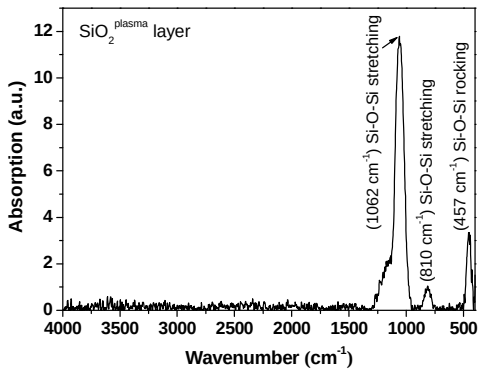

Figure 5. FTIR spectrum of a deposited SiO_2^{plasma} layer of thickness $d_{SiO2plasma}$ = 96 nm.

The FTIR spectrum of SiO_2^{plasma} layer used to cover the AgNPs, in order to complete the plasmonic substrate, is shown in Fig. 5. One can observe the three typical TO modes of molecular vibrations of amorphous silicon dioxide [31]. In particular, the FTIR spectrum shows the Si-O-Si rocking vibration at 457 cm^{-1}, the symmetric stretching mode at 810 cm^{-1}, and the asymmetric stretching mode at 1062 cm^{-1}. The shoulder centered around 1250 cm^{-1}, characteristic of thermal SiO_2 is clearly observable on the spectrum. The lack of Si-H stretching bond at 2250 cm^{-1}, the C-H symmetric stretching bond in CH_3 environment at 2900 cm^{-1}, the C-H asymmetric stretching bond at 2960 cm^{-1} and the OH bonds, both associated at 3450 cm^{-1} and free at 3630 cm^{-1}, that appear in plasma deposited organosilicon layers [32] when only HMDSO is used as precursor, testifies for the efficient process of oxidation and the high quality of the elaborated SiO_2^{plasma} layer. The FTIR spectrum presents a weak shift to lower frequencies in the peak position of the Si-O-Si asymmetric stretching mode, 1062 cm^{-1} instead of 1076 cm^{-1} as expected for thermal SiO_2 layer, most likely due to the slight SiO_2 disorder. Due to the small thickness of SiO_2^{plasma} layer, only 96 nm as measured by spectroscopic ellipsometry, a slight noise in the absorption FTIR spectrum is observed in Fig. 5.

The ellipsometric spectrum of SiO_2^{plasma} layer (Fig. 6) was used to determine the refractive index and the thickness of the layer by applying the Forouhi-Bloomer dispersion low [33] and the obtained values are n = 1.45 (at λ = 632.8 nm) and $d_{SiO2plasma}$ = 96 nm, respectively. The ellipsometric spectrum of SiO_2^{plasma} layer is identic to one of the thermal SiO_2 layer for the same thickness which testifies for the high quality of the plasma deposited silica layer in this study. It means that the layer composition is close to thermal silica one and there is no silver contamination in this layer. In fact, due to the electric field polarization, the ellipsometric measurements are extremely sensitive to changes in the refractive index and the extinction coefficient due to any silver presence inside the SiO_2 matrix. Even a very small fraction of Ag-atoms in the SiO_2 layer leads to a departure in the cosΔ variation, that gives the

phase difference, induced by the reflection, between the perpendicular and parallel components of the polarized electric field.

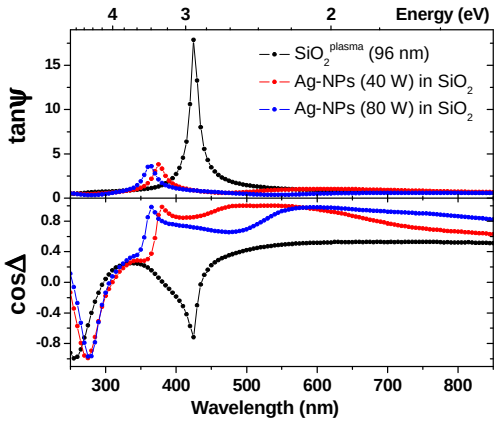

Figure 6. Ellipsometry spectra of elaborated samples: SiO_2^{plasma} layer (black line) and two plasmonic substrates P = 40 and 80 W, t_s = 5 s, and deposition time for the SiO_2^{plasma} coverlayer t_d = 60 s.

To guarantee the performance of plasmonic substrates when integrated in devices one needs to characterize their dielectric response. A good way is to use reliable non-destructive diagnostic methods like ellipsometry and reflectometry. When AgNPs are embedded in the SiO_2 layer, the ellipsometric spectra indicate their presence by shift of the peak to higher energies in the tanΨ variation and by appearance of a peak in the cosΔ variation at the same wavelength as for the tanΨ variation, as shown in Fig. 6 for the two plasmonic substrates presented on the TEM plan-view images in Fig. 4. The tanΨ variation is closely related to changes in the amplitudes of the polarized electric field after reflection. It means that even small variations in the size and density of AgNPs will be detected by spectroscopic ellipsometry. Larger the size of AgNPs, larger the energy shift of their peak on the ellipsometric spectra is. This is an expected behaviour of ellipsometric spectra for AgNPs with different size and density as already presented in other studies [34,35]. Modelling of the recorded ellipsometric spectra, based on the quasi-static approximation of the classical Maxwell-Garnett formalism, however accounting for the electronic confinement effect through the damping parameter, is presented elsewhere [36]. Alternatively to the ellipsometric spectra analysis presented by Oates *at al.* [35] where AgNPs deposited on SiO_2 layer are surrounded by air, the present plasmonic structures appear more complex as the AgNPs are embedded in the SiO_2 matrix and an appropriate description of the dielectric functions of different media and of the interface-related artefacts requires an in-depth analysis.

Visible-UV reflectance spectra are particularly easy to obtain experimentally or model theoretically, and furthermore they display a notable sensitivity to the incorporation of AgNPs in the dielectric matrix, as shown in Figs. 7 and 8.

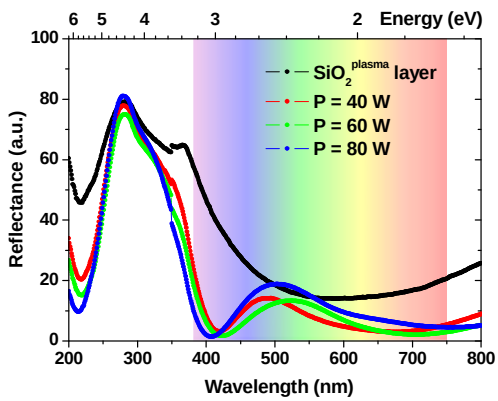

Figure 7. Reflectance spectra of SiO_2^{plasma} layer (thickness $d_{SiO2plasma}$ = 96 nm, black line) and the elaborated plasmonic substrates: the AgNPs delta-layers were deposited with P = 40 W (red line), 60 W (green line) and 80 W (blue line) for fixed sputtering time t_s = 5 s. The deposition time of the SiO_2^{plasma} coverlayer is t_d = 60 s ($d_{SiO2plasma}$ = 13 nm).

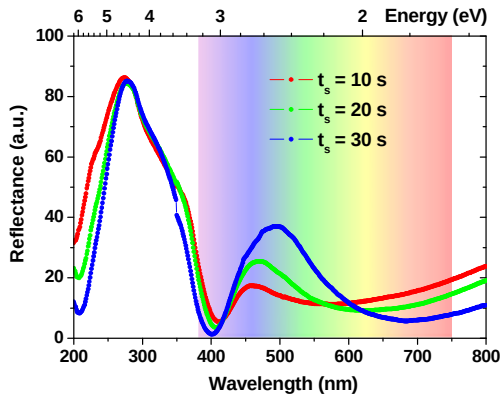

Figure 8. Reflectance spectra of plasmonic substrates: the AgNPs delta-layers were deposited with P = 10 W for increasing sputtering times t_s = 10 s (red line), 20 s (green line), 30 s (blue line). The deposition time of the SiO_2^{plasma} coverlayer is t_d = 30 s ($d_{SiO2plasma}$ = 5 nm).

By changing either the injected power (Fig. 7) or the sputtering time (Fig. 8) one drastically affects the reflectance in the visible range (400 – 750 nm) where most of the potential applications of plasmonic substrates are expected. This enhanced sensitivity is a direct consequence of the design of our specific substrates which allows to simultaneously combine strong absorption at the LSPR (near 413 nm for spherical AgNPs in SiO_2 host matrix) and antireflective effect of the multilayer structure (near 600 nm) [10]. On Figs. 7 or 8, one clearly observes that higher the embedded Ag amount, by increasing the deposition time or the injected power respectively, higher the reflectance in the middle of the visible range is (near 500 nm). One thus expects a high sensitivity in the elastic scattering response for LSPR-sensitive devices or inelastic scattering response for SERS substrates. It is worth to underline here the high sensitivity of the plasma elaborated plasmonic substrates for optical applications in the visible range: the reflectance is modified around 25% (on average) at 500 nm.

5. Conclusions

We have shown how the key parameters of the plasmonic nanostructures (size, density, distance to the surface) can be controlled by tuning the elaboration conditions combining sputtering of silver nanoparticles and plasma polymerization. The proposed plasma deposition method offers the possibility for elaboration, in a reproducible way, of large-area solid plasmonic substrates. The optical response of these composite substrates has shown to be very sensitive to any stimuli that affect the dielectric response at the vicinity of their surface. They thus appear as promising for enhanced spectroscopies based on LSPR or SERS, and for surface-plasmon mediated photocatalytic devices.

Acknowledgments

This work is financially supported by the program IDEX Transversalité of University of Toulouse (ANR-11-IDEX-0002-02), under project ADAGIO. A. P. acknowledges PhD-grant from Université Paul Sabatier, Toulouse under AO3-project BioNAg.

References

[1] Maier S A, Kik P G, H. A. Atwater, S. Meltzer, E. Harel, B. E. Koel and A. G. Requicha 2003 Local detection of electromagnetic energy transport below the diffraction limit in metal nanoparticle plasmon waveguides *Nature Materials* **2** 229-232

[2] Stewart M E, Anderton Ch R, Thompson L B, Maria J, Gray S K, Rogers J A and Nuzzo R G 2008 Nanostructured Plasmonic Sensors *Chem. Rev.* **108** 494-521

[3] Rycenga M, Cobley C M, Zeng J, Li W, Moran C H, Zhang Q, Qin D and Xia Y 2011 Controlling the Synthesis and Assembly of Silver Nanostructures for Plasmonic Applications *Chem. Rev.* **111** 3669-3712

[4] Vo-Dinh T, Yan F and Stokes D L 2005 Plasmonic–Based Nanostructures for Surface-Enhanced Raman Scattering Bioanalysis in "*Protein Nanotechnology: Protocols, Instrumentation, and Applications*" edited by Vo-Dinh T (Humana Press, Totowa, New Jersey, 2005) 255-283

[5] Fleischmann M, Hendra P J and McQuillan A J 1974 Raman spectra of pyridine adsorbed at a silver electrode *Chem. Phys. Lett.* **26** 163-166

[6] Benzo P, Cattaneo L, Farcau C, Andreozzi A, Perego M, Benassayag B, Pécassou B, Carles R and Bonafos C 2011 Stability of Ag nanocrystals synthesized by ultra-low energy ion implantation in SiO_2 matrices *J. Appl. Phys.* 109, 103524

[7] Pal A, Stokes D L, Alarie J-P and Vo-Dinh T 1995 Selective Surface-Enhanced Raman Spectroscopy Using a Polymer-Coated Substrate *Anal. Chem.* **67** 3154-3159

[8] Lacy W B, Williams J M, Wenzler L A, Beebe Jr T P and Harris J M 1996 Characterization of SiO_2-Overcoated Silver-Island Films as Substrates for Surface-Enhanced Raman Scattering *Anal. Chem.* **68** 1003-1011

[9] Carles R, Farcau C, Bonafos C, BenAssayag G, Pécassou B and Zwick A 2009 The synthesis of single layers of Ag nanocrystals by ultra-low-energy ion implantation for large-scale plasmonic structures *Nanotechnology* **20** 355305

[10] Carles R, Farcau C, Bonafos C, BenAssayag G, Bayle M, Benzo P, Groenen J and Zwick A 2011 Three Dimensional Design of Silver Nanoparticle Assemblies Embedded in Dielectrics for Raman Spectroscopy Enhancement and Dark-Field Imaging *ACS NANO* **5** 8774-8782
[11] Bayle M, Benzo P, Combe N, Gatel C, Bonafos C, BenAssayag G and Carles R 2014 Experimental investigation of the vibrational density of states and electronic excitations in metallic nanocrystals *Phys. Rev. B* **89** 195402
[12] Kay E and Hecq M 1984 Metal clusters in plasma polymerized matrices: Gold *J. Appl. Phys.* **55** 370-374
[13] Perrin J, Despax B and Kay E 1985 Optical properties and microstructure of gold–fluorocarbon-polymer composite films *Phys. Rev. B* **32** 719-732
[14] Laurent C and Kay E 1989 Properties of metal clusters in polymerized hydrocarbon versus fluorocarbon matrices *J. Appl. Phys.* **65** 1717-1723
[15] Despax B and Flouttard J L 1989 Synthesis of gold-carbon composites by simultaneous sputtering and plasma polymerization of propane in RF capacitively coupled diode system (13.56 MHz) *Thin Solid Films* **168** 81-88
[16] Despax D and Raynaud P 2007 Deposition of ‘‘Polysiloxane’’ Thin Films Containing Silver Particles by an RF Asymmetrical Discharge *Plasma Process. Polym.* **4** 127-134
[17] Körner E, Fortunato G, Hegemann D 2009 Influence of RF Plasma Reactor Setup on Carboxylated Hydrocarbon Coatings, *Plasma Process. Polym.* **6** 119-125
[18] Dilonardo E, Milella A, Palumbo F, Capitani G, d’Agostino R, Fracassi F 2010 One-Step Plasma Deposition of Platinum Containing Nanocomposite Coatings *Plasma Process. Polym.* **7** 51-58
[19] Kylián O, Choukourov A, Biederman H 2013 Nanostructured Plasma Polymers *Thin Solid Films* **548** 1-17
[20] Drábik M, Pešička J, Biederman H and Hegemann D 2015 Long-term aging of Ag/a-C:H:O nanocomposite coatings in air and in aqueous environment *Sci. Technol. Adv. Mater.* **16** 025005
[21] Saulou C, Despax B, Raynaud P, Zanna S, Marcus P and Mercier-Bonin M 2009 Plasma deposition of organosilicon polymer thin films with embedded nanosilver for prevention of microbial adhesion *Appl. Surf. Sci.* **256S** S35–S39
[22] Körner E, Aguirre M H, Fortunato G, Ritter A, Rühe J and Hegemann D 2010 Formation and Distribution of Silver Nanoparticles in a Functional Plasma Polymer Matrix and Related Ag^+ Release Properties *Plasma Process. Polym.* **7** 619-625
[23] Despax B, Saulou C, Raynaud P, Datas L and Mercier-Bonin M 2011 Transmission electron microscopy for elucidating the impact of silver-based treatments (ionic silver versus nanosilver-containing coating) on the model yeast ***Saccharomyces cerevisiae*** *Nanotechnology* **22** 175101
[24] Alissawi N, Zaporojtchenko V, Strunskus T, Hrkac T, Kocabas I, Erkartal B, Chakravadhanula V S K, Kienle L, Grundmeier G, Garbe-Schönberg, Faupel F 2012 Tuning of the ion release properties of silver nanoparticles buried under a hydrophobic polymer barrier *J. Nanopart. Res.* **14** 928
[25] Pugliara A, Makasheva K, Despax B, Bayle M, Carles R, Benzo P, BenAssayag G, Pécassou B, Sancho M-C, Navarro E, Echegoyen Y, Sanz I, Laborda F and Bonafos C 2014

Toxicity effect on ***Chlamydomonas reinhardtii***: a novel method to study bio-available silver release from a layer of AgNPs embedded in silica matrix *Proc. IEEE Nanotechnology Materials and Devices Conference -IEEE NMDC-*, Aci Castello, Italy.
[26] Ram Prasad G, Daniels S, Cameron D C, McNamara B P, Tully E, O'Kennedy R 2005 PECVD of biocompatible coatings on 316L stainless steel *Surface & Coatings Technology* **200** 1031-1035
[27] Camacho J J, Santos M, Díaz L and Poyato J M L 2008 Optical emission spectroscopy of oxygen plasma induced by IR CO2 pulsed laser *J. Phys. D: Appl. Phys.* **41** 215206
[28] Hegemann D, Vohrer U, Oehr C and Riedel R 1999 Deposition of SiO_x films from O_2/HMDSO plasmas *Surface and Coatings Technology* **116-119** 1033-1036
[29] Aumaille K, Vallée C, Granier A, Goullet A, Gaboriau F and Turban G 2000 A comparative study of oxygen/organosilicon plasmas and thin $SiO_xC_yH_z$ flms deposited in a helicon reactor *Thin Solid Films* **359** 188-196
[30] Goujona M, Belmonte T and Henrion G 2004 OES and FTIR diagnostics of HMDSO/O_2 gas mixtures for SiO_x deposition assisted by RF plasma *Surface and Coatings Technology* **188-189** 756-761
[31] Kirk C T 1988 Quantitative analysis of the effect of disorder-induced mode coupling on infrared absorption in silica *Phys. Rev. B* **38** 1255-1273
[32] Makasheva K, Villeneuve-Faure C, Le Roy S, Despax B, Boudou L, Laurent C and Teyssedre G 2013 Silver nanoparticles embedded in dielectric matrix: charge transport analysis with application to control of space charge formation *Annual Report IEEE Conference on Electrical Insulation and Dielectric Phenomena -CEIDP-* **1** 238-241 DOI: 10.1109/CEIDP.2013.6747079
[33] Forouhi A R and Bloomer I 1986 Optical dispersion relations for amorphous semiconductors and amorphous dielectrics *Phys. Rev. B* **34** 7018-7026
[34] Kreibig U and Vollmer M "*Optical Properties of Metal Clusters*" (Springer Series in Materials Science 25, Springer, Berlin, 1995)
[35] Oates T W H and Mücklich A 2005 Evolution of plasmon resonances during plasma deposition of silver nanoparticles *Nanotechnology* **16** 2606-2611
[36] Pugliara A, Bayle M, Carles R, Bonafos C, Despax B and Makasheva K 2015 Spectroscopic ellipsometry study of the dielectric response of plasmonic structures containing a layer of silver nanoparticles embedded in silica matrix *Proc. E-MRS Spring Meeting 2015*, Lille, France.